Treatment for high-concentration liquid crystal wastewater with a novel Fenton–SBR–microwave pyrolysis integrated process

Jincheng Li, Baoxiu Zhao, Qingpeng Ji, Yanqing Zhang, Kaixin Zhang, Tianshuo Gou, Wenxiang Xia and Jie Liu

ABSTRACT

A novel Fenton–SBR–microwave pyrolysis integrated process is developed to treat liquid crystal wastewater possessing complex components, high toxicity and strong stability. In this integrated process, Fenton–SBR and microwave pyrolysis are for the removal of chemical oxygen demand (COD) and disposal of iron mud generated in the Fenton process respectively. The effects of H_2O_2:Fe^{2+} molar ratio and Fenton dosage on COD removal were optimized. The experimental results revealed that the removal efficiencies for COD and total organic carbon (TOC) were 99.8% and 99.2%, and the values for MLSS and SVI were stable at 4,500 mg L^{-1} and 65%, respectively. Microscopic examination proved that there were *rotifer*, *Epistylis galea*, *Opercularia coarctata*, *vorticella* and *mormon genus* which are indicative microbes for good water quality. Iron mud waste produced in the Fenton reaction was handled with microwave pyrolysis, producing α-Fe_2O_3 commercial byproduct. The estimated cost including chemical reagents and electricity for this integrated process is about \$320 T^{-1}, without consideration of the added value of the α-Fe_2O_3 byproduct. TOC removals in the Fenton and SBR processes both fit well with pseudo-first-order kinetics and the corresponding half-life times are 0.15 and 7 h, respectively.

Key words | COD, Fenton, Fenton–SBR, liquid crystal wastewater, microwave pyrolysis, SBR

Jincheng Li
Baoxiu Zhao (corresponding author)
Qingpeng Ji
Yanqing Zhang
Kaixin Zhang
Tianshuo Gou
Wenxiang Xia
Jie Liu
School of Environmental and Municipal Engineering,
Qingdao University of Technology,
Qingdao 266033,
China
E-mail: *zhaobaoxiu@tsinghua.org.cn*

INTRODUCTION

With the development of organic synthesis, environmental pollution caused by organic pollutants has attracted researchers' attention (Hu *et al.* 2018; Kim *et al.* 2018). The contamination caused by liquid crystal wastewater is typical organic pollution. Alkyl glucoside (Zafiu *et al.* 2016; Amato & Beolchini 2018) or alkyl sulfonate (Srinivasan *et al.* 2019) and surface active agents (Li *et al.* 2016) are the dominant components in liquid crystal wastewater. Many investigations have proved that surface active agents are potential carcinogenic substances to humans (Kasuya & Hatanaka 2016; Xu & Gye 2018). Unfortunately, alkyl sulfonate, perfluorosulfonic acid and phthalate esters diffuse in water worldwide (Hansen *et al.* 2002; Pistocchi & Loos 2009; Zhao & Zhang 2009), and they are even detected in the blood system of human beings (Zhang *et al.* 2010; Poothong *et al.* 2017). Normally, liquid crystal industrial wastewater has four characters: complex components, high chemical oxygen demand (COD) concentration, severe bio-toxicity and low biodegradability.

Now, Fenton and electron-Fenton are the common methods for this special wastewater. Colades *et al.* (2015) treated this wastewater with electron-Fenton and found that COD removal was only 79%, suggesting that advanced oxidation processes could not completely decompose organic pollutants or transformation products. Furthermore, the disposal of iron mud produced in the electron-Fenton reaction was not discussed in their research. Su *et al.* (2013) carried out a fluidized-bed Fenton process to remove monoethanolamine and phosphate in liquid crystal wastewater and found that degradation kinetics for monoethanolamine and phosphate conformed to the first-order reaction. Fenton, or electron-Fenton, is an important treatment for high-concentration liquid crystal wastewater, and organics are degraded by ·OH which has very powerful oxidation and decomposes almost all organic pollutants (Zhao *et al.* 2016). Although Fenton is efficient for this special wastewater, the produced iron mud is a type of hazardous waste and should not be

doi: 10.2166/wst.2019.336

ignored. The higher the concentration of COD, the greater the volume of iron mud that is in the Fenton reaction. Iron mud should be handled in a safe, economical and effective manner. Microwave pyrolysis has many advantages, such as shorter pyrolysis time and lower running cost, compared with conventional pyrolysis (Deng *et al.* 2016; Zhang *et al.* 2018). Furthermore, microwaves have powerful sterilization abilities by destroying the cell structure of harmful microorganisms (Zhang *et al.* 2016; Auksornsri *et al.* 2018). So, it seems that microwave pyrolysis is a friendly disposal technology to realize reduction, resources and harmlessness.

Biological treatment is economical for wastewater which must possess low bio-toxicity and high biodegradability (B/C value) (Kumar *et al.* 2010). Badawy *et al.* (2009) studied the effect of the B/C value on the efficiency of the activated sludge treatment process and found that only 61% COD was removed when the B/C value was lower than 0.25, but 92% COD was removed when it was higher than 0.5. The SBR process is not directly suitable for highly toxic liquid crystal wastewater, as the inhibitory and toxic effects for microbes increase drastically with the concentration of organic wastewater (Tennekes & Sánchez-Bayo 2013; Wang *et al.* 2019). Considering COD removal, economical cost and resource recovery, we performed a novel Fenton–SBR–microwave pyrolysis integrated process in which frontal Fenton–SBR was for wastewater and the following microwave pyrolysis was for iron mud produced in the Fenton reaction.

MATERIALS AND METHODS

Materials

H_2O_2, $FeSO_4{\cdot}7H_2O$, H_2SO_4 and NaOH are all analytical reagents purchased from Tianjin Chemical Reagent Company, China. High purity water (18.2 MΩ cm^{-1}) used in all experiments was prepared with a water purification instrument (Unique-R20, Research Scientific Instruments Company, China). Sludge was withdrawn from the Haibo River sewage treatment plant (Qindao, China), and its concentration and volume index were 8,500 mg L^{-1} and 90%, respectively. The qualities of raw liquid crystal wastewater from the industrial plant were as follows: COD = 150,000 mg L^{-1}, pH = 4.8, BOD = 2,200 mg L^{-1}, T_N = 36 mg L^{-1}, T_P = 5 mg L^{-1}.

Fenton–SBR–microwave pyrolysis hybrid process

Raw liquid crystal wastewater (5 L) was transferred into a conical Fenton pool and the pH value was first adjusted to 3, and then Fenton reagents were added to start the reaction. After 30 min, the Fenton reaction finished. To accelerate the flocculation, the pH value was adjusted to 8 by adding 5 mol L^{-1} NaOH aqueous solution. Clear water from the Fenton pool and the other wastewater from washing cans containing methanol (the quantity of cleaning water almost equalled that of the Fenton outlet in this chemical plant) were mixed and discharged to the SBR pool in which active sludge had been activated for about 24 h. Iron mud from the Fenton pool was withdrawn and concentrated mechanically, and then pyrolyzed by microwaves in a microwave stove (M1-L213B, Midea, China). In the SBR stage, hydrolytic time was controlled at 24 h, initial mixed liquor suspended solids (MLSS) were 4,500 mg L^{-1} and bubbling air was set at 60 mL min^{-1}. To maintain the stability of the SBR process, certain nutrition and phosphorus elements were added. The procedure of the Fenton–SBR–microwave pyrolysis integrated process for wastewater is shown in Figure 1.

Analytical methods

Chemical oxygen demand (COD) was analyzed with a spectrophotometer (Hach-DR 2800, USA) equipped with a digestion instrument (MH-2800D, Hach). Samples were first digested at 150 °C for 2 h in the digestion instrument and then cooled to room temperature. Their concentrations were recorded by the spectrophotometer at 620 nm wavelength. Before analysis, all samples were diluted to satisfy the detection range. Total organic carbon (TOC) was analyzed by a TOC analyzer (TOC-4200, Shimadzu, Japan) connected to an automatic sampler system, and N_2 was the carrier gas. All samples were also diluted to satisfy the calibration method. The crystal phase of Fe_2O_3 was analyzed via its X-ray diffraction (XRD) pattern, which was monitored using a D/max RB system (Cu Kα_1 irradiation, $\lambda = 1.5406$ Å, voltage = 40 kV, current = 30 mA, scanning rate = 0.01°/s, scanning range = 10°–80°).

RESULTS AND DISCUSSION

Fenton process

The Fenton dosage and molar ratio of Fe^{2+} to H_2O_2 ($m Fe^{2+}$: $m H_2O_2$) were investigated and their effects on COD removal are displayed in Figure 2(a) and 2(b). From Figure 2(a), it is observed that COD removal increases with the enhancement of Fe^{2+} concentration (namely

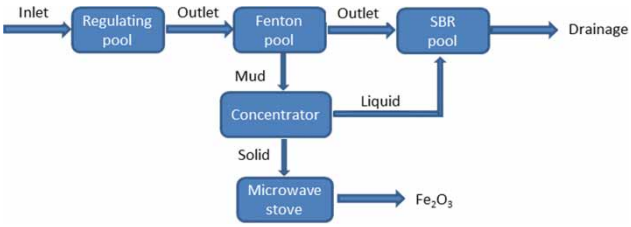

Figure 1 | Technical procedure of the Fenton–SBR–microwave pyrolysis integrated process for high-concentration liquid crystal wastewater.

Fenton dosage), and almost 95% COD is removed when the Fe^{2+} concentration is 0.3 mol L^{-1}. The reason is because the more Fenton is added, the more ·OH radicals are produced. The reaction equations are as follows: $Fe^{2+} + H_2O_2 + H^+ \rightarrow Fe^{3+} + \cdot OH$, $\cdot OH + \text{pollutants} \rightarrow \text{intermediates}$. From Figure 2(b) it can be seen that COD removal is first enhanced and then decreases with the enhancement of $m Fe^{2+}$:$m H_2O_2$, and the optimal value of $m Fe^{2+}$:$m H_2O_2$ is 1:3. When $m Fe^{2+}$:$m H_2O_2$ is lower than 1:3, more HO· radicals are produced and remain, resulting in higher COD removal. However, when $m Fe^{2+}$:$m H_2O_2$ is higher than 1:3, more excessive Fe^{2+} ions react with HO· radicals, forming a disputed state between Fe^{2+} and organic pollutants with HO· (Vorontsov 2019), so COD removal declines.

Liquid crystal wastewater is a type of special industrial wastewater, which has high toxicity and complex components. Other methods for this special wastewater are listed in Table 1. It is observed that Fenton is the most popular method and it is significant in handling high-concentration liquid crystal wastewater, however, a biological method, such as MBR, is only for low-concentration liquid crystal wastewater.

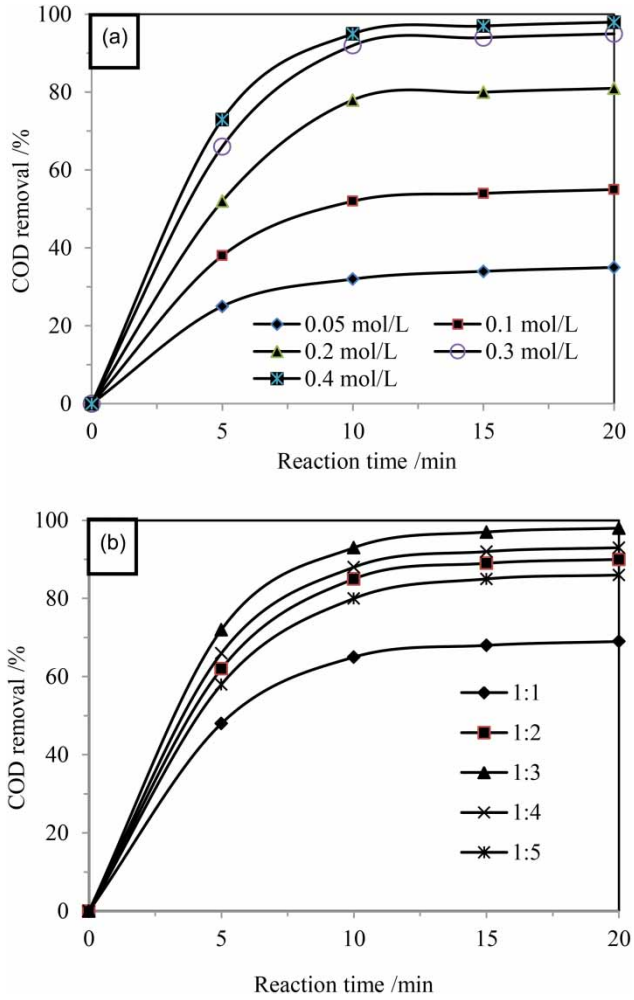

Figure 2 | (a) Effect of Fe^{2+} concentration on COD removal, where $m[Fe^{2+}]$:$m[H_2O_2] = 1:3$, pH = 3. (b) Effect of $m[Fe^{2+}]$:$m[H_2O_2]$ on COD removal, where $[Fe^{2+}] = 0.3$ mol L^{-1}, pH = 3.

SBR process

Water qualities, including COD, TOC, biochemical oxygen demand (BOD) and T_N and T_P, were analyzed before starting the SBR process, and the values were as follows: COD = 2,300 mg L^{-1}, BOD = 932 mg L^{-1}, TOC = 3,386 mg L^{-1}, T_N = 28 mg L^{-1}, T_P = 3 mg L^{-1}. It is observed that the ratio of BOD to COD climbed from 0.015 at the beginning to 0.41 after the Fenton process, revealing that treated water from the Fenton process is biodegradable. To analyze the running stability of the SBR process, COD removal, mixed liquid suspended solids (SSLV) and sludge volume index (SVI) were measured, respectively, and the results are presented in Figure 3. It is observed that 90% COD is removed, suggesting that the SBR process is stable and credible. Besides water qualities, the activated sludge is also analyzed. It can be seen that the concentration of SSLV decreases firstly before ten running cycles and then increases slowly to the original state after 19 running cycles. Furthermore, the variation trend of SVI is similar to that of SSLV, as shown in Figure 3(b). Here, the hydraulic residence time (HRT) of every cycle is 24 h. Before the first ten cycles, the microbes in the activated sludge received a sudden impact from the liquid crystal wastewater, forming a serious inhibition and resulting in depopulation, so the values of SSLV and SVI both decline. After ten cycles, organisms grew slowly and reached a stable period. Coincidentally it was found that the sludge became compact at the beginning, forming numerous micelles; however, it became looser after several running times and changed to denser again in the later stage.

Table 1 | Other methods and results for liquid crystal wastewater

Methods	Operating conditions	Results
Adsorption (Ligaray *et al.* 2018)	COD = 1,348 mg L^{-1}, pH = 4, HRT = 20.3 h, T = 30 °C	COD removal = 73.3%
E-Fenton (Colades *et al.* 2015)	COD = 6,481 mg L^{-1}, $[Fe^{2+}]$ = 5.125 mM, $[H_2O_2]$ = 325 mM, current = 1.5 A, pH = 1.95	COD removal = 79%
MBR (Wu *et al.* 2013)	COD = 150 mg L^{-1}, F/M ratio <0.4, pH = 7, DO >3 mg L^{-1}, T = 27 ± 2 °C	COD removal = 86%, nitrogen removal = 84%
Fluidized-bed Fenton (Su *et al.* 2013)	$[Fe^{2+}]$ = 3 mM, $[H_2O_2]$ = 50 mM, pH = 3	MEA removal = 76%
Zero-valent iron reduction (Lee *et al.* 2009)	BOD/COD = 0.5, SS = 4,000 mg L^{-1}, iodine = 30 mg L^{-1}, HRT = 30 d, pH = 6.3, T = 30 °C	COD removal >90%, SS = 350 mg L^{-1}

Microscopic examination

The dominant microbes existing in the activated sludge were identified with a high-power inverted microscope (XDY-100, New Optics Company, China); see Figure 4. The representative microbes were metazoans such as flagellates, *Arcella* and spiral worm in active sludge, as shown in Figures 4(a1)–4(a2) and S1 (flagellates' video

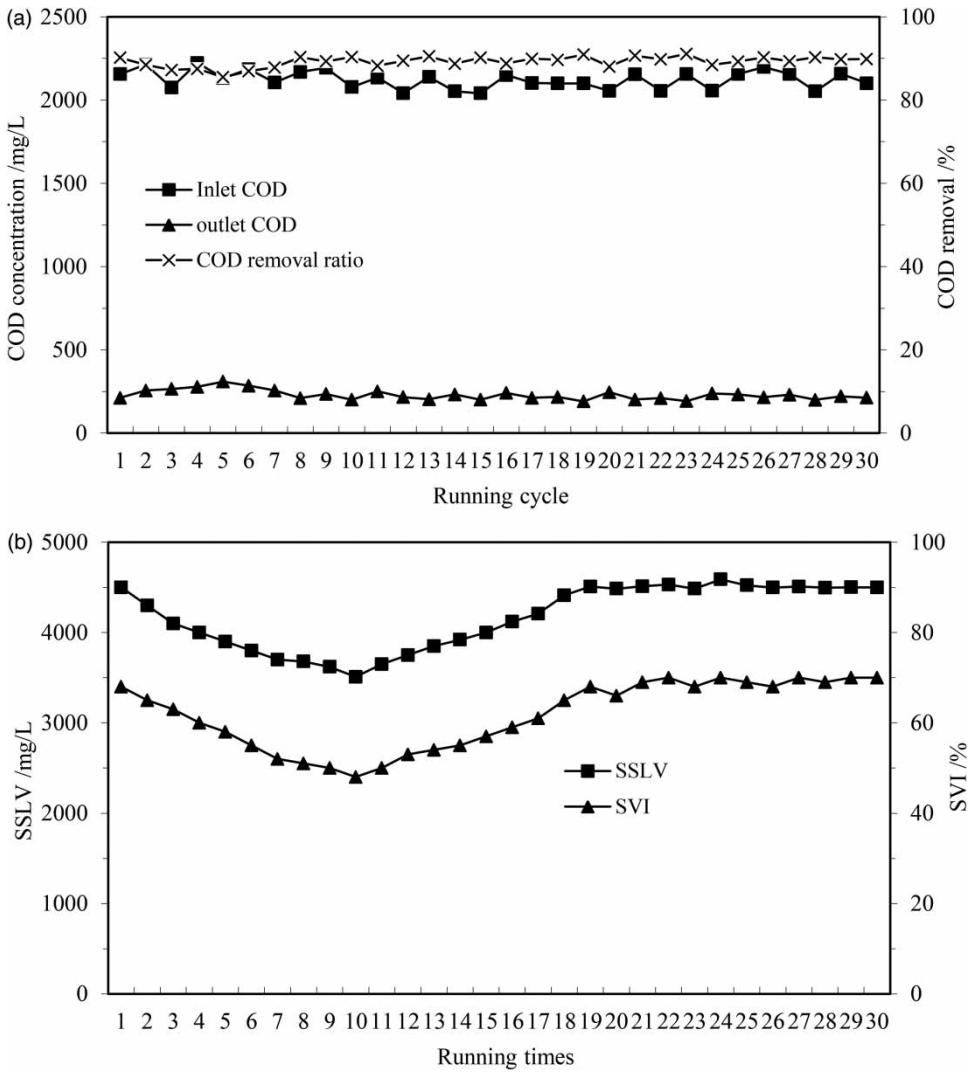

Figure 3 | (a) COD concentrations of inlet and outlet and its removal ratio in the SBR process. (b) The change of SSLV and SVI in the SBR process.

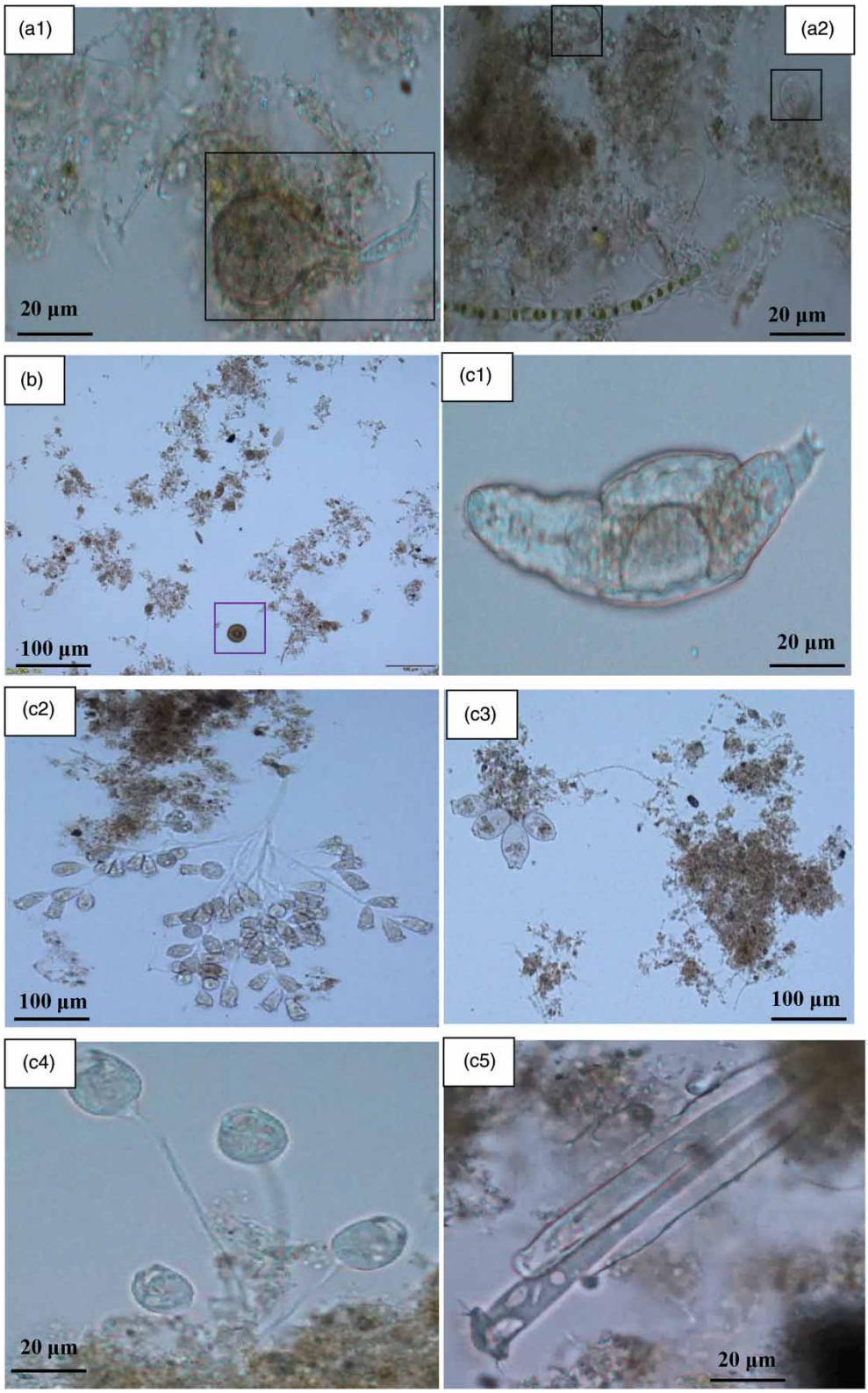

Figure 4 | (a) Microscopic photographs of flagellates (a1) and spiral worm (a2) in activated sludge. (b) Microscopic photograph of activated sludge at the second running cycle. The black point surrounded by a square is an *Arcella*'s corpse. (c) Microscopic photographs of activated sludge mainly populated by rotifer (c1), *Epistylis galea* (c2), *Opercularia coarctata* (c3), *Vorticella* (c4) and mormon genus (c5) in a stable SBR process.

presented in the Supplementary Material), and the probable reason is that the activated sludge was withdrawn from the aeration tank, which was mainly occupied by metazoans. Furthermore, there are micelles in the activated sludge, showing that the biological activity of sludge is perfect. However, at the beginning of the SBR process, sludge-loading increased so suddenly that some metazoans could not endure the attack of pollutant, resulting in the decline of activity (there is an *Arcella* corpse identified within a purple square in Figure 4(b)). Compared with the standard microorganism, the microbes of Figure 4(c1)–4(c5) are assigned to rotifer, *Epistylis galea*, *Opercularia coarctata*, *Vorticella* and mormon worm (a kind of amoeba) in turn. Here, *Epistylis galea*, *Opercularia coarctata*, *Vorticella* and mormon worm can secrete many extracellular polymeric substances, which is good for the formation of micelles and the flocculation of activated sludge, so the above-mentioned microbes are regarded as the characteristic indicator organisms to evaluate the successful operation of the SBR process in many wastewater treatment plants. Li *et al.* (2013) studied the effects of *Vorticella* and rotifer on aerobic sludge granules in an SBR reactor and found that *Vorticella* anchored into the granules by stalks, while rotifer attached or adhered to the surface of the granules. The attachment and accumulation both improved the features of the sludge, thus the values of SSLV and SVI both picked up again, showing that the flower shape of rotifer and branch shape of *Opercularia coarctata* and *Epistylis galea* have important roles in the recovery of sludge, proved by Li's research. Furthermore, there was an abundance of rotifers and mormon worm after the 20th cycle; S2 and S3 in the Supplementary Material are videos of mormon worm and rotifers recorded by microscope in this stage. In fact they only appear in good water quality, indicating that the water quality is much improved.

Microwave pyrolysis

Microwaves are a kind of electromagnetic wave and can excite polar materials to form a high-temperature field where the crystal phase transformation can be immediately completed. Zhao *et al.* (2015) successfully synthesized β-Ga_2O_3 photocatalyst using the microwave-assisted hydrothermal method. Fortunately, iron is a good substance for absorbing microwaves. Iron mud containing dominant $Fe(OH)_3$ was treated by microwave pyrolysis and the effects of microwave time and power on pyrolysis were studied. The results are presented in Figure 5(a). An

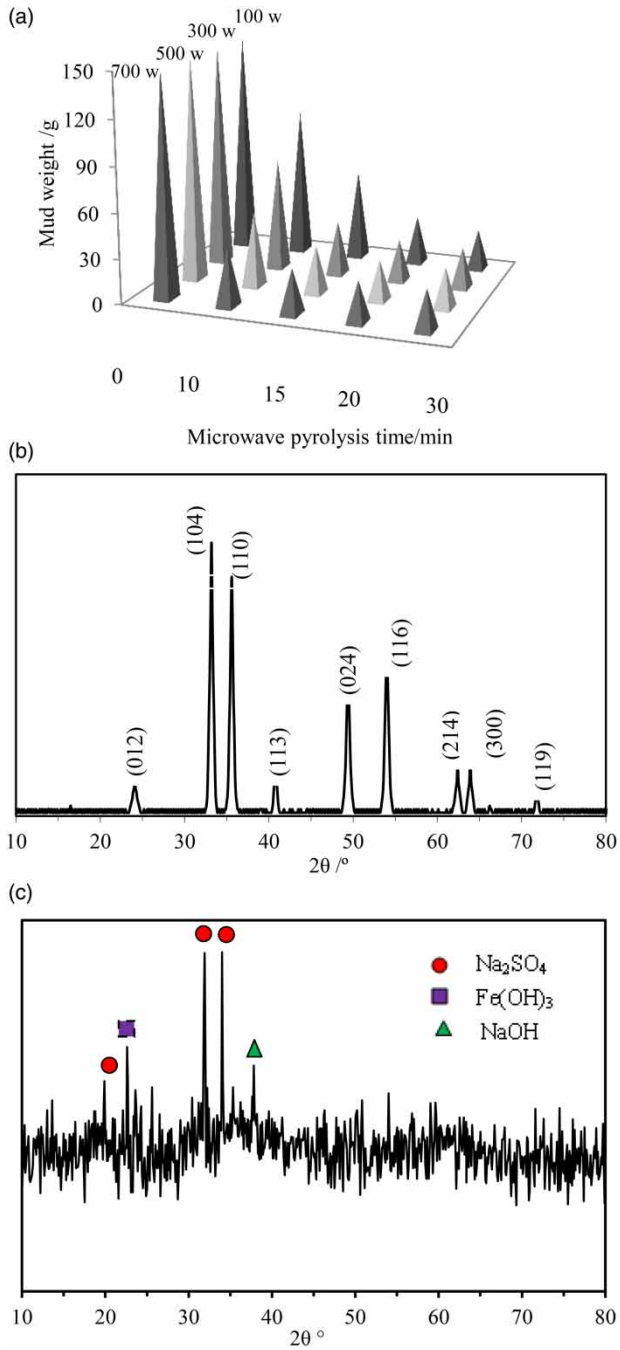

Figure 5 | (a) The effects of microwave power and time on the weight of iron slag. (b) The XRD pattern of α-Fe_2O_3 obtained by microwave pyrolysis where microwave power = 300 W, microwave time = 20 min. (c) The XRD pattern of raw iron mud from the Fenton reaction.

obvious conclusion that iron mud weight decreases with the enhancement of microwave irradiation time and power can be achieved from this 3-D figure. Because a high-temperature field is formed during the microwave pyrolysis process, $Fe(OH)_3$ as a kind of polar material absorbs microwaves quickly and forms Fe_2O_3 by losing

crystal water. The corresponding reaction equation is: $Fe(OH)_3 \rightarrow Fe_2O_3 + H_2O$.

To confirm this conclusion, Fe_2O_3 was purified several times with alcohol–water aqueous solution (alcohol: water = 1:1) and characterized by XRD analysis. The XRD pattern is displayed in Figure 5(b). It is clear that the crystal phase of Fe_2O_3 belongs to the α-phase, for there appear apparently characteristic diffraction peaks for the (012), (104), (110), (113), (024), (116), (018), (214) and (119) crystal planes of the rhombohedral phase of α-Fe_2O_3 crystalline structure (JCPDS No. 33-0664). No additional peaks of any other impurities were identified in this figure, suggesting that α-Fe_2O_3 is the only byproduct of microwave pyrolysis. Marinho *et al.* (2014) coincidentally prepared α-Fe_2O_3 nanorods by the microwave heating method; α-Fe_2O_3 was extracted from iron mud via microwave pyrolysis, realizing the effective recovery of waste resources. It is valuable for microwave pyrolysis not only to avoid environmental pollutants but also to obtain an efficient and commercial recovery for the α-Fe_2O_3 byproduct.

It is apparent that α-Fe_2O_3 is the sole product from clear iron mud pyrolyzed by microwaves, according to Figure 5(b). In fact, there are other ingredients in raw iron mud generated from the Fenton reaction, such as NaOH, $FeSO_4$ and Na_2SO_4. To make certain of the probable components in raw iron mud, XRD of raw iron mud was carried out and is displayed in Figure 5(c). Compared with standard diffraction peaks, Na_2SO_4, $Fe(OH)_3$ and NaOH were identified. Na_2SO_4 and $Fe(OH)_3$ both come from the Fenton reaction, and NaOH is from pH adjustment.

TOC removal kinetics

TOC removals in the Fenton–SBR process were analyzed and the results are displayed in Figure 6(a) and 6(b). It can be seen that TOC decreases quickly in the Fenton process, illustrating that Fenton is an efficient method for liquid crystal wastewater. At optimal conditions, 76.8% TOC is removed by the Fenton process within 0.33 h and 87.2% TOC is removed by the SBR process within 24 h; see Figure 6(b). TOC declines from 50,000 to 398 mg L^{-1}. Furthermore, TOC removal kinetics in the Fenton and SBR processes were investigated and the results are displayed in Figure 6(c). From this figure, it is observed that TOC removals in Fenton peroxidation and SBR processes both fit with pseudo-first-order kinetics, and the reaction rate constants were 4.608 and 0.098 h^{-1}, respectively. The corresponding half-life time is 0.15 and 7 h for Fenton and SBR processes, respectively, on which basis TOC removal can be easily forecast in actual treatment for wastewater.

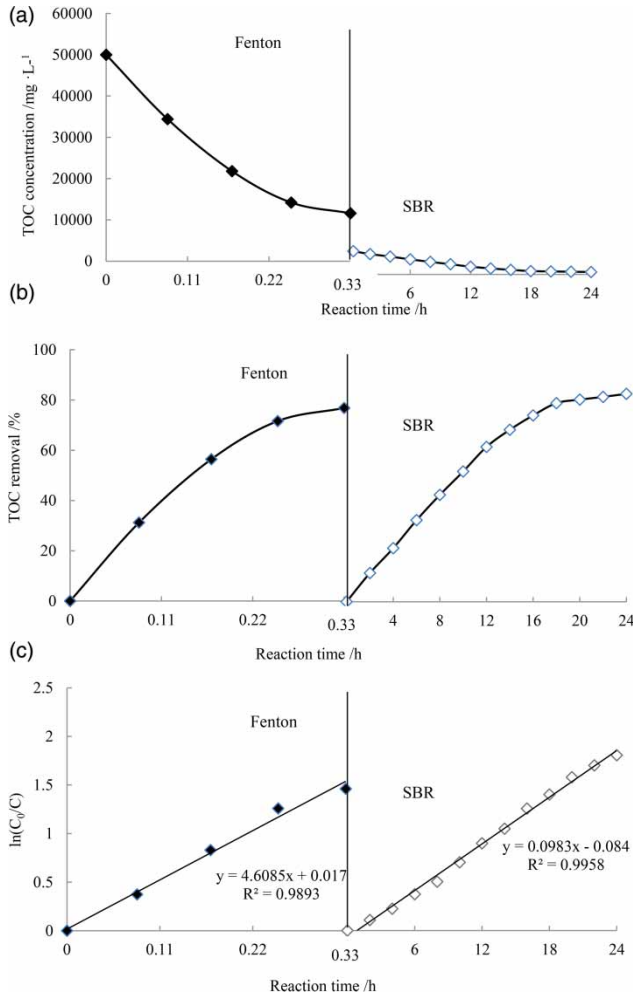

Figure 6 | (a) TOC concentrations in Fenton and SBR processes, respectively. (b) TOC removals in Fenton and SBR processes, respectively. (c) The linear relationships between ln (C_0/C) and reaction time t in Fenton and SBR processes, respectively, where: in the Fenton process, $[Fe^{2+}] = 0.3$ mol L^{-1}, pH = 3, $m[Fe^{2+}]:m[H_2O_2] = 1:3$; in the SBR process, SSLV = 4,500 mg L^{-1}, SVI = 65%, TOC initial concentrations in Fenton and SBR processes are 50,000 and 3,386 mg L^{-1}, respectively.

Cost analysis

Except for the costs of instrument and labor, the fees for chemical reagents and electricity charge for the Fenton–SBR–microwave pyrolysis integrated process were calculated. In the Fenton process, the cost mainly focuses on chemical reagents such as H_2O_2, $FeSO_4 \cdot 7H_2O$, H_2SO_4 and NaOH, and in SBR and microwave pyrolysis the main cost is electricity. The estimated cost of this Fenton–SBR–microwave

pyrolysis integrated process is approximately US$320 per ton of wastewater.

CONCLUSIONS

High-concentration liquid crystal wastewater was efficiently and safely decomposed by the Fenton–SBR–microwave pyrolysis integrated process, where not only wastewater was degraded by the Fenton–SBR process but also iron mud was handled by microwave pyrolysis, realizing liquid–solid synchronous treatment.

ACKNOWLEDGEMENTS

This work was financially supported by Shandong Provincial Natural Science Foundation (Nos. ZR2016EEM15, ZR2019MEE097) and The National Water Pollution Control and Treatment Science and Technology Major Project (No. 2017ZX07101-002-05). Furthermore, we especially thank Prof. Rogers-Carpenter for the revision in English grammar and sentence structure.

SUPPLEMENTARY MATERIAL

S1, S2 and S3 are uploaded on the following youtube address: https://www.youtube.com/channel/UC9elA_h-AlsrjBVMK6lEYxQ.

REFERENCES

Amato, A. & Beolchini, F. 2018 End of life liquid crystal displays recycling: a patent review. *J. Environ. Manage.* **225**, 1–9.

Auksornsri, T., Tang, J., Tang, Z., Lin, H. & Songsermpong, S. 2018 Dielectric properties of rice model food systems relevant to microwave sterilization process. *Innov. Food Sci. Emerg. Technol.* **45**, 98–105.

Badawy, M. I., Wahaab, R. A. & El-Kalliny, A. S. 2009 Fenton-biological treatment processes for the removal of some pharmaceuticals from industrial wastewater. *J. Hazard. Mater.* **167**, 567–574.

Colades, J. I., de Luna, M. D. G., Su, C. C. & Lu, M. C. 2015 Treatment of thin film transistor-liquid crystal display (TFT-LCD) wastewater by the electro-Fenton process. *Separ. Purif. Technol.* **145**, 104–112.

Deng, S., Wang, P., Zhang, G. & Dou, Y. 2016 Polyacrylonitrile-based fiber modified with thiosemicarbazide by microwave irradiation and its adsorption behavior for Cd(II) and Pb(II). *J. Hazard. Mater.* **307**, 64–72.

Hansen, K. J., Johnson, H. O., Eldridge, J. S., Butenhoff, J. L. & Dick, L. A. 2002 Quantitative characterization of trace levels of PFOS and PFOA in the Tennessee River. *Environ. Sci. Technol.* **36** (8), 1681–1685.

Hu, L., Zhang, G., Liu, M., Wang, Q. & Wang, P. 2018 Enhanced degradation of Bisphenol A (BPA) by peroxymonosulfate with Co_3O_4-Bi_2O_3 catalyst activation: effects of pH, inorganic anions, and water matrix. *Chem. Eng. J.* **338**, 300–310.

Kasuya, M. C. & Hatanaka, K. 2016 Cytotoxicity and cellular uptake of perfluorocarboxylic acids. *J. Fluor. Chem.* **188**, 1–4.

Kim, H. I., Wijenayake, J. J., Mohapatra, D. & Rout, P. C. 2018 A process to recover high purity iodine in wastewater from liquid crystal display (LCD) manufacturing industry. *Hydrometallurgy* **181**, 91–96.

Kumar, A., Dhall, P. & Kumar, R. 2010 Redefining BOD:COD ratio of pulp mill industrial wastewaters in BOD analysis by formulating a specific microbial seed. *Int. Biodeter. Biodegrad.* **64** (3), 197–202.

Lee, W., Cha, D. K., Oh, Y. K., Ko, K. B. & Song, J. S. 2009 Zero-valent iron pretreatment for detoxifying iodine in liquid crystal display (LCD) manufacturing wastewater. *J. Hazard. Mater.* **164** (1), 67–72.

Li, J., Ma, L., Wei, S. & Horn, H. 2013 Aerobic granules dwelling vorticella and rotifers in an SBR fed with domestic wastewater. *Separ. Purif. Technol.* **110**, 127–131.

Li, S., Zhang, G., Wang, P., Zheng, H. & Zheng, Y. 2016 Microwave-enhanced Mn-Fenton process for the removal of BPA in water. *Chem. Eng. J.* **294**, 371–379.

Ligaray, M., Futalan, C. M., de Luna, M. D. & Wan, M. W. 2018 Removal of chemical oxygen demand from thin-film transistor liquid-crystal display wastewater using chitosan-coated bentonite: isotherm, kinetics and optimization studies. *J. Clean. Prod.* **175**, 145–154.

Marinho, J. Z., Montes, R. H. O., de Moura, A. P., Longo, E., Varela, J. A., Munoz, R. A. A. & Lima, R. C. 2014 Rapid preparation of α-FeOOH and α-Fe_2O_3 nanostructures by microwave heating and their application in electrochemical sensors. *Mater. Res. Bull.* **49**, 572–576.

Pistocchi, A. & Loos, R. 2009 A map of European emissions and concentrations of PFOS and PFOA. *Environ. Sci. Technol.* **43** (24), 9237–9244.

Poothong, S., Thomsen, C., Padilla-Sanchez, J. A., Papadopoulou, E. & Haug, L. S. 2017 Distribution of novel and well-known poly- and perfluoroalkyl substances (PFASs) in human serum, plasma, and whole blood. *Environ. Sci. Technol.* **51** (22), 13388–13396.

Srinivasan, R., Nambi, I. M. & Senthilnathan, J. 2019 Liquid crystal display electrode assisted bio-reactor for highly stable and enhanced biofilm attachment for wastewater treatment – a sustainable approach for e-waste management. *Chem. Eng. J.* **358**, 1012–1021.

Su, C. C., Chen, C. M., Anotai, J. & Lu, M. C. 2013 Removal of monoethanolamine and phosphate from thin-film transistor liquid crystal display (TFT-LCD) wastewater by the fluidized-bed Fenton process. *Chem. Eng. J.* **222**, 128–135.

Tennekes, H. A. & Sánchez-Bayo, F. 2013 The molecular basis of simple relationships between exposure concentration and toxic effects with time. *Toxicology* **309**, 39–51.

Vorontsov, A. V. 2019 Advancing Fenton and photo-Fenton water treatment through the catalyst design. *J. Hazard. Mater.* **372**, 103–112.

Wang, S., Yan, L. C., Zheng, S. S., Li, T. T., Fan, L. Y., Huang, T., Li, C. & Zhao, Y. H. 2019 Toxicity of some prevalent organic chemicals to tadpoles and comparison with toxicity to fish based on mode of toxic action. *Ecotoxicol. Environ. Saf.* **167**, 138–145.

Wu, Y. J., Whang, L. M., Chang, M. Y., Fukushima, T., Lee, Y. C., Cheng, S. S., Hsu, S. F., Chang, C. H., Shen, W., Yang, C. Y., Fu, R. & Tsai, T. Y. 2013 Impact of food to microorganism (F/M) ratio and colloidal chemical oxygen demand on nitrification performance of a full-scale membrane bioreactor treating thin film transistor liquid crystal display wastewater. *Bioresour. Technol.* **141**, 35–40.

Xu, Y. & Gye, M. C. 2018 Developmental toxicity of dibutyl phthalate and citrate ester plasticizers in *Xenopus laevis* embryos. *Chemosphere* **204**, 523–534.

Zafiu, C., Hussain, Z., Küpcü, S., Masutani, A., Kilickiran, P. & Sinner, E.-K. 2016 Liquid crystals as optical amplifiers for bacterial detection. *Biosens. Bioelectron.* **80**, 161–170.

Zhang, T., Wu, Q., Sun, H. W., Zhang, X. Z., Yun, S. H. & Kannan, K. 2010 Perfluorinated compounds in whole blood samples from infants, children, and adults in China. *Environ. Sci. Technol.* **44** (11), 4341–4347.

Zhang, H., Tang, Z., Rasco, B., Tang, J. & Sablani, S. S. 2016 Shelf-life modeling of microwave-assisted thermal sterilized mashed potato in polymeric pouches of different gas barrier properties. *J. Food Eng.* **183**, 65–73.

Zhang, H., Gao, Z., Liu, Y., Ran, C., Mao, X., Kang, Q., Ao, W., Fu, J., Li, J., Liu, G. & Dai, J. 2018 Microwave-assisted pyrolysis of textile dyeing sludge, and migration and distribution of heavy metals. *J. Hazard. Mater.* **355**, 128–135.

Zhao, B. & Zhang, P. 2009 Photocatalytic decomposition of perfluorooctanoic acid with β-Ga_2O_3 wide bandgap photocatalyst. *Cataly. Commun.* **10** (8), 1184–1187.

Zhao, B., Li, X., Yang, L., Wang, F., Li, J., Xia, W., Li, W., Zhou, L. & Zhao, C. 2015 β-Ga_2O_3 nanorod synthesis with a one-step microwave irradiation hydrothermal method and its efficient photocatalytic degradation for perfluorooctanoic acid. *Photochem. Photobiol.* **91**, 42–47.

Zhao, B., Wang, X., Shang, H., Li, X., Li, W., Li, J., Xia, W., Zhou, L. & Zhao, C. 2016 Degradation of trichloroacetic acid with an efficient Fenton assisted TiO_2 photocatalytic hybrid process: reaction kinetics, byproducts and mechanism. *Chem. Eng. J.* **289**, 319–329.

First received 23 May 2019; accepted in revised form 18 September 2019. Available online 14 October 2019